CONTROL OF MICROMACHINED DEFORMABLE MIRRORS

M.L. Agronin, R. Bartman, F.Y. Hadaegh, W. Kaiser
Jet Propulsion Laboratory
California Institute of Technology
Pasadena, CA 91109-8099

P.K.C. Wang
Department of Electrical Engineering
University of California
Los Angeles, CA 90024

Abstract:

A micromachined deformable mirror with pixelated electrostatic actuators is proposed. The paper begins with a physical description of the proposed mirror. Then a mathematical model in the form of a nonlinear partial differential equation describing the mirror surface deformations is derived. This model is used to derive the required voltages for the actuators to achieve a specified static deformation of the mirror surface. This is followed by the derivation of a static nonlinear feedback controller for achieving noninteracting actuation. Then the structure for a complete control system for wavefront correction is proposed. The paper concludes with a discussion of the physical implementation of the proposed control system.

1. INTRODUCTION

In the development of large space interferometers and multi-aperture reflectors, deformable mirrors are used to compensate for distortions in elements of the optical train and/or in the instrument's field of view. Such mirrors should be small and lightweight. Moreover, they should be highly pixelated so that the deformations can be controlled with high lateral resolution.

The first actively controlled deformable mirrors were developed by NASA in the 1960's for use as solar collectors or as ground-based telescopes [1]. Since then, there has been extensive development in this area. Comprehensive surveys of works on actively controlled deformable mirrors were given by Ealey [2] and Tyson [3]. In 1977, Grosso and Yellin [4] developed a membrane mirror whose deformations are controlled by means of discrete electrostatic actuators. Subsequently, various forms of deformable mirrors with discrete piezoelectric and magnetostrictive actuators were also developed [5]-[9]. The advent of silicon VLSI technology has made possible the integration of deformable mirrors with microelectronic circuitry. In 1983, Hornbeck [10] perfected a deformable mirror device with pixelated mirror elements whose size is 51 μm square. The mirror deformations are controlled by electrostatic actuators driven by microelectronic circuits which are integrated with the mirror assembly. His mirror was used primarily as a light modulator. Later, in 1989, a wavefront control device with a deformable mirror integrated with control and sensor units was introduced by Ealey and Wheeler [11]. In their device, the actuators are spaced 1.0 mm apart. The voltages applied to the actuators are on the order of 200 volts. Recently, efforts have been initiated at the Jet Propulsion Laboratory in exploiting micromachining technology to develop deformable mirrors with the aforementioned characteristics and with pixelated electrostatic actuators which are spaced less than 25 microns apart. In this paper, attention is focused on the analytical design of control systems for such deformable

mirrors.

The paper begins with a physical description of the proposed mirror. Then a mathematical model in the form of a nonlinear partial differential equation describing the mirror surface deformations is derived. This equation is used to derive the required actuator voltages to achieve a specified static deformation of the mirror surface. This is followed by the derivation of a static nonlinear feedback controller for achieving noninteracting actuation. Then the structure for a complete control system for wavefront correction is proposed. The paper concludes with a discussion of the physical implementation of the proposed control system.

2. PHYSICAL DESCRIPTION OF DEFORMABLE MIRROR

Figures 1 and 2 show respectively the sketches of the top and side views of the proposed deformable mirror with pixelated capacitive actuators. The mirror may be realized as "flip chip"-type assemblies consisting of two matched micromachined silicon structures mounted face-to-face and fused together along their peripheries. The key elements of the mirror consist of simple, easily replicated, electrostatic linear actuators, each responsible for pulling on a small portion of a thin flexible silicon membrane which is the substrate for the deformable mirror. The mirror surface is formed by depositing a metallic or multi-layer dielectric film on the membrane. The membrane with posts (See Fig. 2) is micromachined from a silicon sheet. The posts serve as supports for the membrane and also as halves of the electrostatic actuators. The bottom half of the mirror assembly consists of a set of posts with four silicon blades attached to each post. These blades serve as leaf springs for supporting the posts of the upper mirror assembly, and for providing a restoring force for the actuation system. This bottom assembly is micromachined from a silicon wafer. The electrostatic actuators are formed by attaching conductive pads to the upper posts and the bottom half of the mirror assembly. The electronic element access, electronic actuator drivers, and possibly the feedback controller circuitry may be monolithically integrated into the mirror assembly.

We note that the geometric structure of the deformable mirror proposed here differs from that of Hornbeck [10]. In his mirror, each actuator, when activated, produces a concave deformation of the mirror surface over the entire pixel. This causes focusing of the incoming light beam in front of the pixel. Here, each actuator pulls down on the mirror surface at a post area and thereby induces deformation over adjacent portions of the mirror surface. Except for the flat spots over the post areas, the overall shape of the mirror surface is determined by the displacements of all the actuators.

The initial performance goals for the proposed mirror will be the control of a 32 × 32 pixel flat mirror with 10 nm accuracy. Once these goals have been achieved, efforts will be directed at extending the number of pixels/control elements until 10 nm accuracy can be achieved over a 1024 × 1024 pixel surface.

3. MATHEMATICAL MODEL

Let Ω be an open connected subset of the Euclidean plane R^2 with a piecewise smooth boundary $\partial\Omega$ representing the spatial domain of the mirror. We introduce a mesh on Ω whose mesh points are denoted by $\mathbf{x}_{mn} = (x_{1m}, x_{2n})$, $m = 1,\ldots,M$; $n = 1,\ldots,N$. For a rectangular mirror, Ω is

specified by $\Omega_R = \{(x_1,x_2) \in R^2: |x_1| \le \ell_1, |x_2| \le \ell_2\}$, where the ℓ_i's are specified lengths. For a circular mirror, Ω is specified by the disk $\Omega_C = \{(r,\theta), 0 \le r \le r_o, 0 \le \theta \le 2\pi\}$. At each mesh point $\mathbf{x}_{mn}$, we introduce a patch Ω_{mn}, a bounded open subset of Ω representing the effective spatial domain of the (m,n)-th actuator force containing $\mathbf{x}_{mn}$ as an interior point. Typical meshes and patches for the rectangular and circular mirrors are shown in Fig. 3.

Let the mirror surface be a thin membrane with density $\rho = \rho(\mathbf{x})$ being a specified positive piecewise smooth function satisfying the following bounds:

$$0 < \rho_{min} \le \rho(\mathbf{x}) \le \rho_{max} < +\infty \quad \text{for all } \mathbf{x} \in \Omega. \tag{1}$$

The variation of the mass density due to the supporting posts can be included in ρ by setting $\rho(\mathbf{x}) = \rho_{mn}$ (a known constant) for $\mathbf{x} \in \Omega_{mn}$.

Let σ_{ij}, $i,j = 1,2$ denote the components of the symmetric stress tensor in the mirror surface satisfying the positivity condition

$$c_1\|\zeta\|^2 \le \sum_{i=1}^{2}\sum_{j=1}^{2} \sigma_{ij}\xi_i\xi_j \le c_2\|\xi\|^2 \quad \text{for all } \xi = (\xi_1,\xi_2) \in R^2, \tag{2}$$

where c_1 and c_2 are known positive constants. In the special case with uniform tension T, we have $\sigma_{ij} = T\delta_{ij}$, where δ_{ij} denotes the Kronecker delta.

The downward displacement $u(t,\mathbf{x})$ normal to the mirror surface at a point $\mathbf{x} \in \Omega$ and time $t \ge 0$ can be described by the following equation:

$$\rho(\mathbf{x})\frac{\partial^2 u}{\partial t^2} - \sum_{i=1}^{2}\sum_{j=1}^{2}\frac{\partial}{\partial x_i}\left(\sigma_{ij}(\mathbf{x})\frac{\partial u}{\partial x_j}\right) = f, \tag{3}$$

where $f = f(t,\mathbf{x})$ is the surface force density whose explicit form will be derived later. Assuming that the mirror is rigidly attached to its boundary $\partial\Omega$, u must satisfy the boundary condition

$$u(t,\mathbf{x}) = 0 \text{ for } \mathbf{x} \in \partial\Omega \text{ and } t \ge 0. \tag{4}$$

Finally, the initial conditions for u are specified by

$$u(0,\mathbf{x}) = u_o(\mathbf{x}), \quad \frac{\partial u}{\partial t}(t,\mathbf{x}) = u_o'(\mathbf{x}) \quad \text{for } \mathbf{x} \in \Omega. \tag{5}$$

To derive an explicit expression for the surface force density f, we first consider the electrostatic force density over a patch Ω_{mn} due to a specified voltage $V_{mn}(t)$ applied to the (m,n)-th actuator. We assume that the mirror surface curvature is small so that each patch Ω_{mn} is essentially parallel to the bottom assembly. Thus each actuator's conductive surfaces can be regarded as making up a parallel-plate capacitor. Neglecting fringing effects of the electric field at the boundary of Ω_{mn}, the electrostatic force density is given by

$$f_e(t,\mathbf{x}) = \frac{1}{2}\varepsilon_o\left(\frac{V_{mn}(t)}{D - u(t,\mathbf{x}_{mn})}\right)^2 \quad \text{for all } \mathbf{x} \in \Omega_{mn}, \tag{6}$$

where D is the distance between the undeformed mirror surface and the bottom plane and ε_o is the permittivity of free space. When $D \gg |u(t,\mathbf{x}_{mn})|$, (6) can be approximated by

$$f_e(t,\mathbf{x}) = \frac{1}{2}\varepsilon_o V_{mn}^2(t)/D^2 \quad \text{for all } \mathbf{x} \in \Omega_{mn}. \tag{6'}$$

Considering each leaf spring as a small cantilever beam having uniform cross section with moment of inertia I and Young's modulus E, the force density f_s due to four leaf springs over the patch Ω_{mn} is given by

$$f_s(t,\mathbf{x}) = \frac{12EI}{\ell_{mn}^3 A_{mn}} u(t,\mathbf{x}_{mn}) \quad \text{for all } \mathbf{x} \in \Omega_{mn}, \tag{7}$$

where A_{mn} denotes the area of the patch Ω_{mn}. Here, we have neglected the inertial effects of the leaf springs.

Let ϕ_{mn} denote the spatial weighting function associated with the (m,n)-th actuator such that $\phi_{mn}(\mathbf{x}) = 0$ for $\mathbf{x} \in \Omega - (\Omega_{mn} \cup \partial\Omega_{mn})$. Combining (6) and (7), equation (3) becomes a nonlinear partial differential equation given by

$$\rho(\mathbf{x})\frac{\partial^2 u}{\partial t^2} - \sum_{i=1}^{2}\sum_{j=1}^{2}\frac{\partial}{\partial x_i}\left(\sigma_{ij}(\mathbf{x})\frac{\partial u}{\partial x_j}\right)$$
$$= \sum_{m=1}^{M}\sum_{n=1}^{N}\left\{\frac{1}{2}\varepsilon_o\left(\frac{V_{mn}(t)}{D - u(t,\mathbf{x}_{mn})}\right)^2 - \frac{12EI}{\ell_{mn}^3 A_{mn}}u(t,\mathbf{x}_{mn})\right\}\phi_{mn}(\mathbf{x}). \tag{8}$$

Let $K(\mathbf{x},\mathbf{x}',t,\tau)$ denote the Green's function corresponding to the solution of the linear equation:

$$\rho(\mathbf{x})\frac{\partial^2 u}{\partial t^2} - \sum_{i=1}^{2}\sum_{j=1}^{2}\frac{\partial}{\partial x_i}\left(\sigma_{ij}(\mathbf{x})\frac{\partial u}{\partial x_j}\right) = \delta(t-\tau,\mathbf{x}-\mathbf{x}'), \tag{9}$$

with boundary and initial conditions given by (4) and (5), where δ denotes the Dirac delta function at $t = \tau$ and $\mathbf{x} = \mathbf{x}'$. Equation (8) can be reformulated as a nonlinear integral equation:

$$u(t,\mathbf{x}) = \int_\Omega K(\mathbf{x},\mathbf{x}',t,0)u_o(\mathbf{x}')\,d\mathbf{x}' + \int_\Omega \frac{\partial K}{\partial t}(\mathbf{x},\mathbf{x}',t,0)u_o'(\mathbf{x}')\,d\mathbf{x}'$$
$$+\int_0^t\int_\Omega K(\mathbf{x},\mathbf{x}',t,\tau)\sum_{m=1}^{M}\sum_{n=1}^{N}\left\{\frac{1}{2}\varepsilon_o\left(\frac{V_{mn}(t)}{D - u(t,\mathbf{x}_{mn})}\right)^2 - \frac{12EI}{\ell_{mn}^3 A_{mn}}u(t,\mathbf{x}_{mn})\right\}\phi_{mn}(\mathbf{x}')d\mathbf{x}' \tag{10}$$

Under the assumption that the mirror deformations over Ω_{mn} are sufficiently small compared to D so that (6) may be approximated by (6'), equations (8) and (10) become linear. This assumption may not be justified when D is made small so as to reduce the operating voltage

levels of the actuators. For example, in Hornbeck's deformable mirror, D is 620 nm, and the peak mirror deformation for normal operation is around 100 nm. Evidently, (6') is not a good approximation for this case.

4. STATIC SHAPE CONTROL

Let $u_d = u_d(\mathbf{x})$ be the desired static shape of the mirror surface defined over the entire spatial domain Ω. It is required to determine the static voltages V_{mn} for each actuator to achieve the desired shape u_d. Let $K_s = K_s(\mathbf{x},\mathbf{x}')$ denote the Green's function associated with the boundary-value problem:

$$\sum_{i=1}^{2}\sum_{j=1}^{2}\frac{\partial}{\partial x_i}\left(\sigma_{ij}(\mathbf{x})\frac{\partial u}{\partial x_j}\right) = \delta(\mathbf{x}-\mathbf{x}'), \quad \mathbf{x}\in\Omega, \tag{11}$$

with boundary condition

$$u(\mathbf{x}) = 0 \quad \text{for } \mathbf{x}\in\partial\Omega. \tag{12}$$

Then, the static equation corresponding to (8) can be reformulated as an integral equation for the mirror displacement u corresponding to given static actuator voltages $\bar{V}_{mn}$:

$$u(\mathbf{x}) = \int_\Omega K_s(\mathbf{x},\mathbf{x}')\sum_{m=1}^{M}\sum_{n=1}^{N}\left\{\frac{1}{2}\varepsilon_o\left(\frac{\bar{V}_{mn}}{D-u(\mathbf{x}_{mn})}\right)^2 - \frac{12EI}{\ell_{mn}^3 A_{mn}}u(\mathbf{x}_{mn})\right\}\phi_{mn}(\mathbf{x}')d\mathbf{x}',$$

$$\text{for } \mathbf{x}\in\Omega. \tag{13}$$

Let $\mathbf{u} = (u(\mathbf{x}_{11}),\ldots,u(\mathbf{x}_{1N}),\ldots,u(\mathbf{x}_{M1}),\ldots,u(\mathbf{x}_{MN}))^T$ and $\bar{\mathbf{V}}^k = (\bar{V}^k_{11},\ldots,\bar{V}^k_{1N},\ldots,\bar{V}^k_{M1},\ldots,\bar{V}^k_{MN})^T$, k = 1,2. Setting $\mathbf{x} = \mathbf{x}_{ij}$ in (13) leads to a set of M × N algebraic equations relating $\mathbf{u}$ and $\bar{\mathbf{V}}^2$. These equations can be written as

$$(\mathbf{I}+\mathbf{K})\mathbf{u} = \mathbf{P}(\mathbf{u})\bar{\mathbf{V}}^2, \tag{14}$$

where $\mathbf{I}$ denotes the MN × MN identity matrix; $\mathbf{K}$ is the MN × MN matrix whose k-th row $\mathbf{K}_k$ is given by

$$\mathbf{K}_k = (K^{ij}_{11},\ldots,K^{ij}_{1N},\ldots,K^{ij}_{M1},\ldots,K^{ij}_{MN}),\ i = \text{integer}(k/M),\ j = k\ \text{Mod}(M), \tag{15}$$

where

$$K^{ij}_{mn} = \left\{\int_{\Omega_{mn}} K_s(\mathbf{x}_{ij},\mathbf{x}')\,\phi_{mn}(\mathbf{x}')\,d\mathbf{x}'\right\}\frac{12EI}{\ell_{mn}^3 A_{mn}}. \tag{16}$$

$\mathbf{P}(\mathbf{u})$ is the MN × MN matrix whose k-th row is $(p^{ij}_{11}(\mathbf{u}),\ldots,p^{ij}_{1N}(\mathbf{u}),\ldots,p^{ij}_{M1}(\mathbf{u}),\ldots,p^{ij}_{MN}(\mathbf{u}))$, where

$$p^{ij}_{mn}(\mathbf{u}) = \frac{\varepsilon_o}{2(D-u(\mathbf{x}_{mn}))^2}\left\{\int_{\Omega_{mn}} K_s(\mathbf{x}_{ij},\mathbf{x}')\,\phi_{mn}(\mathbf{x}')\,d\mathbf{x}'\right\},$$

$$i = \text{integer}(k/M),\ j = k\ \text{Mod}(M). \tag{17}$$

Explicit expressions for K_s and p_{mn}^{ij} corresponding to rectangular and circular mirrors are given in the Appendix.

If we set $\mathbf{u} = \mathbf{u}_d \triangleq (u_d(\mathbf{x}_{11}),\ldots,u_d(\mathbf{x}_{1N}),\ldots,u_d(\mathbf{x}_{M1}),\ldots, u_d(\mathbf{x}_{MN}))^T$, then (14) becomes a set of $M \times N$ linear algebraic equations for the unknown actuator voltages $\bar{\mathbf{V}}$. Evidently, if $\mathbf{P}(\mathbf{u}_d)$ is nonsingular, then $\bar{\mathbf{V}}^2$ is uniquely determined by

$$\bar{\mathbf{V}}^2 = \mathbf{P}(\mathbf{u}_d)^{-1}(\mathbf{I} + \mathbf{K})\mathbf{u}_d. \tag{18}$$

The matrix $\mathbf{P}(\mathbf{u}_d)$ is nonsingular if and only if its rows are linearly independent, or equivalently the $M \times N$ matrices given by

$$\mathbf{P}_{ij}(\mathbf{u}_d) \triangleq \begin{bmatrix} p_{11}^{ij}(u_d) & \cdots & p_{1N}^{ij}(u_d) \\ \vdots & & \vdots \\ p_{M1}^{ij}(u_d) & \cdots & p_{MN}^{ij}(u_d) \end{bmatrix}, \quad i = 1,\ldots,M;\ j = 1,\ldots,N, \tag{19}$$

are linearly independent. Since p_{mn}^{ij} depends on the desired mirror surface displacement $\mathbf{u}_d$, the set $\mathcal{D}$ of all displacements $\mathbf{u}_d$ such that $\mathbf{P}(\mathbf{u}_d)$ is nonsingular corresponds to the set of all mirror surface displacements which have one-to-one correspondence with the actuator voltages $\bar{V}_{mn}$. In fact, if we define the nonlinear mapping $\mathbf{u} \rightarrow N(\mathbf{u})$ by $N(\mathbf{u})=\mathbf{P}(\mathbf{u})^{-1}(\mathbf{I} + \mathbf{K})\mathbf{u}$, then N is an invertible mapping with domain $\mathcal{D}$. In the case where the desired mirror surface deformation $u_d = u_d(\mathbf{x})$ has spatial symmetry, the number of equations in (14) can be reduced accordingly.

Now, given a set of actuator voltages $\bar{\mathbf{V}}$, the corresponding mirror surface displacements at the mesh points $\mathbf{x}_{mn}$ can be determined by solving the nonlinear equation (14) for $\mathbf{u}$. If we define the nonlinear mapping $\mathbf{u} \rightarrow \mathcal{N}(\bar{\mathbf{V}}^2)\mathbf{u}$ by $\mathcal{N}(\bar{\mathbf{V}}^2)\mathbf{u} = \mathbf{P}(\mathbf{u})\bar{\mathbf{V}}^2 - \mathbf{K}\mathbf{u}$, then the solutions correspond to the fixed points of $\mathcal{N}(\bar{\mathbf{V}})$. In physical situations where the actuator voltages satisfy a magnitude constraint of the form $\bar{V}_{mn}^2 \le \bar{V}_{max}^2 < \infty$, the set of all admissible $\bar{\mathbf{V}}$'s is given by $\mathcal{V} = \{\bar{\mathbf{V}} \in R^{MN}: \bar{V}_{mn}^2 \le \bar{V}_{max}^2,\ m = 1,\ldots,M,\ n = 1,\ldots,N\}$ (a hypercube in R^{MN}). Then the set of all admissible $\mathbf{u}_d$'s is given by $N^{-1}(\mathcal{V})$.

Remarks:

(R-1) Once the required actuator voltages $\bar{V}_{mn}$ for achieving the desired static mirror surface displacements at the mesh points are determined, the mirror surface displacements at other points in the spatial domain Ω can be found using (13) with $u(\mathbf{x}_{mn})$ set to $u_d(\mathbf{x}_{mn})$.

(R-2) In all the existing works on deformable mirrors, it is assumed that the static mirror surface displacements at the mesh points $\mathbf{x}_{mn}$ are related to the actuator inputs by a linear transformation commonly called the influence function matrix which is valid for small

displacements. For large mirror displacements, the relation between $u(\mathbf{x}_{ij})$ and the actuator voltages $\bar{V}_{mn}$ is given by (13) with $\mathbf{x}$ set to $\mathbf{x}_{ij}$. This relation is implicit and nonlinear. In the special case of small displacements such that approximation (6') holds, this relation becomes linear. Using (13) with a single actuator at Ω_{mn} to obtain $u(\mathbf{x})$ in terms of $\bar{V}_{mn}$ gives the usual influence function.

(R-3) If the number of actuators is less than the number of mesh points at which the desired mirror displacements are specified, then, under the linear approximation (6'), (14) consists of a set of overdetermined linear algebraic equations for the unknown variables $\bar{V}^2_{mn}$. We may use the least-squares solution, which corresponds to obtaining the pseudo-inverse of the influence function matrix [3].

Noninteracting Actuation:

Due to stress in the membrane, the voltage $\bar{V}_{mn}$ applied to the (m,n)-th actuator will influence the membrane displacements at all the patch locations. To simplify the mirror deformation control, it is desirable to introduce appropriate feedback and new control variables c_{mn} such that c_{mn} only influences the mirror displacement u at the mesh point $\mathbf{x}_{mn}$, and $u(\mathbf{x}_{mn})$ only depends on c_{mn}. Thus, the new controls c_{mn} produce noninteracting actuation of the mirror surface displacements at the mesh points. To achieve noninteraction, we introduce a static feedback control of the form $\bar{V}^2 = \mathbf{F}(\mathbf{c} - \mathbf{u})$, where $\mathbf{F}$ is a feedback gain matrix which may depend on $\mathbf{u}$. Thus, in view of (14), we have

$$(\mathbf{I} + \mathbf{K})\mathbf{u} = \mathbf{P}(\mathbf{u})\mathbf{F}(\mathbf{c} - \mathbf{u}), \tag{20}$$

or

$$[\mathbf{I} + (\mathbf{I} + \mathbf{K})^{-1}\mathbf{P}(\mathbf{u})\mathbf{F}]\mathbf{u} = (\mathbf{I} + \mathbf{K})^{-1}\mathbf{P}(\mathbf{u})\mathbf{F}\mathbf{c}, \tag{21}$$

where $\mathbf{c} = (c_{11},\ldots,c_{1N},\ldots,c_{M1},\ldots,c_{MN})^T$. To achieve noninteracting actuation, we seek an MN × MN matrix $\mathbf{F}$ such that $(\mathbf{I} + \mathbf{K})^{-1}\mathbf{P}(\mathbf{u})\mathbf{F} = \Lambda$, a specified constant diagonal matrix with nonzero diagonal elements λ_{ii}. Thus, $\mathbf{u}$ and $\mathbf{c}$ are related by a diagonal matrix operator given by

$$\mathbf{u} = [\mathbf{I} + \Lambda]^{-1}\Lambda\mathbf{c}, \tag{22}$$

and the required feedback gain matrix $\mathbf{F}$ is given by

$$\mathbf{F} = \mathbf{P}(\mathbf{u})^{-1}(\mathbf{I} + \mathbf{K})\Lambda. \tag{23}$$

In physical terms, the static feedback control in effect cancels the spring coupling forces to produce noninteracting actuation with respect to the new control $\mathbf{c}$. In the special case where the mirror displacements are small as compared to the actuator gap D so that approximation (6') is valid, $\mathbf{P}$ becomes a constant matrix. Consequently, $\mathbf{F}$ is also a constant matrix and the noninteracting controller is linear. We note that $\mathbf{P}(\mathbf{u})$ and $\mathbf{K}$ depend on the parameters E, I, D, and ℓ_{mn} whose values can be accurately estimated. Therefore $\mathbf{F}$ can be determined with good accuracy. Finally, the foregoing noninteracting controller is also valid for the

dynamic case, since the couplings between the mirror displacements at the mesh points involve elastic forces only.

5. DYNAMIC SHAPE CONTROL

Assuming that the desired nominal static-shape $\mathbf{u}_d$ for the mirror is attainable by appropriate choices of the actuator voltages $\bar{V}_{mn}$, it is of interest to control the deviations of the mirror shape about $\mathbf{u}_d$ for wavefront correction. We propose to achieve this objective in three steps. Figure 4 shows the proposed structure of the overall control system for wavefront correction. First, a static feedback controller for achieving the desired nominal static mirror-shape and noninteracting actuation of the deformable mirror is introduced. The function of the minor-loop feedback controller is to modify the dynamic response of the actuators. This modification can also be performed ahead of the static feedback controller depending on the method of implementation. Finally, a global feedback controller which makes use of the output of the wavefront estimator to generate the appropriate actuating signals for wavefront correction is introduced. The static feedback controller has already been discussed in Sec. 4. In what follows, the discussion will be devoted to the modification of the dynamic response of the actuator, and the global shape controller for wavefront correction.

5.1 Actuator Dynamics Modification

The main objective here is to modify the dynamics of the actuator to ensure satisfactory response to input commands. Since this controller is to be integrated with the mirror assembly, the control law should have the following properties:

(i) It should be sufficiently simple so that it can be realized by microelectronic circuitry which can be integrated monolithically with the mirror microstructure.
(ii) It should be model independent so that it is unnecessary to identify the system parameters for their implementation.
(iii) Its performance should be sufficiently robust with respect to system parameter variations.

Since the mirror surface has very little internal damping, the actuator forces may induce undesirable surface vibrations. Therefore, it is necessary to introduce damping externally. A possible approach is to introduce external passive damping. This may be achieved by housing the bottom mirror assembly in an enclosure which contains air, and has minute holes for air passage. Alternatively, damping can be achieved by means of active feedback controls.

To derive appropriate forms for the active feedback controls, we make use of the partial differential equation (8) linearized about the nominal mirror surface deformation $\hat{u}_d = \hat{u}_d(\mathbf{x})$ produced by the static actuator voltage $\bar{\mathbf{V}}$ which produces the desired $\mathbf{u}_d$. Note that $\hat{u}_d(\mathbf{x}) = u_d(\mathbf{x})$ only at the mesh points $\mathbf{x} = \mathbf{x}_{mn}$. Let $\delta u = u - \hat{u}_d$, and $\delta \mathbf{V} = \mathbf{V} - \bar{\mathbf{V}}$. The linearized equation (8) is given by

$$\rho(\mathbf{x}) \frac{\partial^2 \delta u}{\partial t^2} - \sum_{i=1}^{2} \sum_{j=1}^{2} \frac{\partial}{\partial x_i} \left(\sigma_{ij}(\mathbf{x}) \frac{\partial \delta u}{\partial x_j} \right)$$

$$= \sum_{m=1}^{M}\sum_{n=1}^{N}\left\{\left(\frac{\varepsilon_o \bar{V}_{mn}^2}{(D - u_d(\mathbf{x}_{mn}))^3} - \frac{12EI}{\ell^3 A_{mn}}\right)\delta u(t,\mathbf{x}_{mn}) + \frac{\varepsilon_o \bar{V}_{mn}\delta V_{mn}(t)}{(D - u_d(\mathbf{x}_{mn}))^2}\right\}\phi_{mn}(\mathbf{x}), \tag{24}$$

with boundary condition

$$\delta u(t,\mathbf{x}) = 0 \text{ for } \mathbf{x} \in \partial\Omega \text{ and } t \geq 0, \tag{25}$$

and initial conditions:

$$\delta u(0,\mathbf{x}) = u_o(\mathbf{x}) - u_d(\mathbf{x}), \quad \frac{\partial \delta u}{\partial t}(0,\mathbf{x}) = u_o'(\mathbf{x}) \text{ for } \mathbf{x} \in \Omega. \tag{26}$$

Consider the total energy functional of the perturbed mirror surface about u_d given by

$$\mathcal{E} = \frac{1}{2}\int_\Omega \left\{\rho(\mathbf{x})\left(\frac{\partial \delta u}{\partial t}\right)^2 + T\left[\left(\frac{\partial \delta u}{\partial x_1}\right)^2 + \left(\frac{\partial \delta u}{\partial x_2}\right)^2\right]\right\} d\mathbf{x}$$

$$- \frac{1}{2}\int_\Omega \sum_{m=1}^{M}\sum_{n=1}^{N}\left(\frac{\varepsilon_o \bar{V}_{mn}^2}{(D - u_d(\mathbf{x}_{mn}))^3} - \frac{12EI}{\ell^3 A_{mn}}\right)(\delta u(t,\mathbf{x}))^2 \phi_{mn}(\mathbf{x})\, d\mathbf{x}. \tag{27}$$

This energy functional is nonnegative for all δu and $\partial \delta u/\partial t$ in the Sobolev space $H_0^1(\Omega)$ (i.e. the Hilbert space of all real-valued square integrable functions defined on Ω and vanishing on $\partial\Omega$ such that their first-order partial derivatives are also square integrable), if

$$\frac{\varepsilon_o \bar{V}_{mn}^2}{(D - u_d(\mathbf{x}_{mn}))^3} < \frac{12EI}{\ell^3 A_{mn}} \quad \text{for } m = 1,\ldots,M,\ n = 1,\ldots,N. \tag{28}$$

The time rate-of-change of $\mathcal{E}$, after integration by parts, and making use of (24) and boundary condition (25), is given by

$$d\mathcal{E}/dt = \int_\Omega \frac{\partial \delta u}{\partial t}\left(\sum_{m=1}^{M}\sum_{n=1}^{N}\left\{\left(\frac{\varepsilon_o \bar{V}_{mn}^2}{(D - u_d(\mathbf{x}_{mn}))^3} - \frac{12EI}{\ell^3 A_{mn}}\right)[\delta u(t,\mathbf{x}_{mn}) - \delta u(t,\mathbf{x})]\right.\right.$$

$$\left.\left. + \frac{\varepsilon_o \bar{V}_{mn}\delta V_{mn}(t)}{(D - u_d(\mathbf{x}_{mn}))^2}\right\}\phi_{mn}(\mathbf{x})\right) d\mathbf{x} \tag{29}$$

By requiring that $\delta u(t,\mathbf{x}) = \delta u(t,\mathbf{x}_{mn})$ and $\partial \delta u(t,\mathbf{x})/\partial t = \partial \delta u(t,\mathbf{x}_{mn})/\partial t$ for all $\mathbf{x} \in \Omega_{mn}$, (29) reduces to

$$d\mathcal{E}/dt = \sum_{m=1}^{M}\sum_{n=1}^{N}\frac{\varepsilon_o \bar{V}_{mn}\delta V_{mn}(t)}{(D - u_d(\mathbf{x}_{mn}))^2}\left\{\int_{\Omega_{mn}}\phi_{mn}(\mathbf{x})\, d\mathbf{x}\right\}\frac{\partial \delta u(t,\mathbf{x}_{mn})}{\partial t}. \tag{30}$$

If we set

$$\delta V_{mn}(t) = -\gamma_{mn}\frac{\partial \delta u}{\partial t}(t,\mathbf{x}_{mn})\,\phi_{mn}(\mathbf{x}), \quad \gamma_{mn} > 0, \tag{31}$$

then

$$d\mathcal{E}/dt = -\sum_{m=1}^{M}\sum_{n=1}^{N} \frac{\varepsilon_o \bar{V}_{mn}\gamma_{mn}}{(D - u_d(\mathbf{x}_{mn}))^2}\left\{\int_{\Omega_{mn}} \phi_{mn}(\mathbf{x})\, d\mathbf{x}\right\}(\partial\delta u(t,\mathbf{x}_{mn})/\partial t)^2 \le 0. \quad (32)$$

The control law (31) implies local rate-feedback at each actuator location with feedback gain $-\gamma_{mn}$ only.

Incorporating the foregoing local rate-feedback with the noninteracting controller, the transfer function between $\mathbf{u}$ and $\mathbf{c}$ is a diagonal matrix $\mathbf{H}(s)$ whose diagonal elements have the form:

$$h_{ii}(s) = \frac{g_i}{(s^2 + 2\zeta_i\omega_i s + \omega_i^2)}, \quad i = 1,\ldots,NM. \quad (33)$$

To achieve zero steady-state error for step actuator commands, a proportional-plus-integral minor-loop controller is introduced. The parameters of the controller and the gain g_i are chosen to ensure stability and satisfactory transient response to step-input commands. When the noninteracting controls are implemented by means of a digital computer, processing delays are introduced. These time-delays may be incorporated in $h_{ii}(s)$.

5.2 Global Controller for Wavefront Correction

The initial step in wavefront correction is to estimate the wavefront of the incoming light wave reflected from the deformable mirror based on the output of the wavefront sensor. In physical situations, a wavefront sensor such as the Hartmann-Shack wavefront sensor uses an array of micro-lenses, each of which samples a portion of the incoming beam and focuses light onto a detector consisting of a CCD camera or a lateral field-effect photodiode array.

Let Ω_s be a bounded open connected subset of R^2 corresponding to the effective spatial domain of the wavefront sensor. We introduce a mesh on Ω_s whose mesh points are denoted by $\hat{\mathbf{x}}_{mn} = (\hat{x}_{1m}, \hat{x}_{2n})$, $m = 1,\ldots,\hat{M}$; $n = 1,\ldots,\hat{N}$. At each mesh point $\hat{\mathbf{x}}_{mn}$, we introduce a patch Ω_s^{mn}, a bounded open subset of Ω_s, representing the effective aperture of the (m,n)-th lenslet containing $\hat{\mathbf{x}}_{mn}$ as an interior point. Let $\Psi = \Psi(t,\hat{\mathbf{x}})$ denote the wavefront of the incoming wave reflected from the deformable mirror and impinging onto the wavefront sensor. The local gradient or angular tilt in the wavefront averaged over the aperture of the (m,n)-th lenslet is given by

$$\overline{\nabla\Psi(t,\cdot)}\Big|_{\mathbf{x}_{mn}} \triangleq \int_{\Omega_s^{mn}} \psi_{mn}(\mathbf{x})\nabla\Psi(t,\mathbf{x})\, d\mathbf{x} = f^{-1}(\hat{\mathbf{x}} - \hat{\mathbf{x}}^o_{mn}), \quad (34)$$

where ψ_{mn} is a given spatial weighting function associated with the (m,n)-th lenslet; f is the focal length of the lenslet; $\hat{\mathbf{x}}^o_{mn}$ is the nominal position of the focal spot for a collimated beam, and $\mathbf{x}$ is the position of the focal spot for the incoming beam. Thus, the angular tilt in the wavefront can be estimated by measuring the deviations $(\hat{\mathbf{x}} - \hat{\mathbf{x}}^o_{mn})$. From the local gradient data, it is possible to obtain an estimate of the

wavefront $\Psi = \Psi(t,\hat{\mathbf{x}})$ [12]. For wavefront sensors with circular apertures, it is advantageous to express Ψ in terms of Zernike polynomials. By comparing Ψ with a reference wavefront Ψ_R, we obtain the wavefront error $\delta\Psi = \Psi_R - \Psi$. In order to generate the mirror shape correction command from $\delta\Psi$, it is necessary to map the wavefront sensor domain Ω_s onto the mirror domain Ω. Let this mapping be a diffeomorphism $\mathbf{S}$ from Ω_s onto Ω. Then the mirror shape correction command $\delta\mathbf{c}$ is obtained by evaluating $\delta C(t,\mathbf{x}) \triangleq \delta\Psi(t,\mathbf{S}^{-1}\mathbf{x})$ at all the actuator locations $\mathbf{x}_{mn}$ in Ω. Again, due to the presence of processing delays in the wavefront estimator, a dynamic compensator may be incorporated in the global shape controller to ensure overall system stability.

6. PHYSICAL IMPLEMENTATION

In the physical implementation of the proposed control system, it is desirable to integrate as much as possible the electronic circuitry of the controllers with the mirror assembly. Due to the minute capacitances associated with the actuators, it is clear that the actuator drivers consisting of operational amplifiers must be located in the immediate vicinities of the actuators.

To implement the rate-feedback control given by (31) for damping, consider a parallel-plate capacitor driven by an operational amplifier as shown in Fig. 5. Assume that the distance Δ between the capacitor plates is time varying so that the capacitance $C(t) = \varepsilon_o A/\Delta(t)$, where A is the area of each plate. Thus, we have

$$C(t)\frac{dv(t)}{dt} + v(t)\frac{dC(t)}{dt} = i(t), \tag{35}$$

where i is the current flowing to the capacitor. Using the expression for $C(t)$, (35) can be rewritten as

$$\frac{\varepsilon_o A}{\Delta(t)}\frac{dv}{dt} - \frac{\varepsilon_o A}{\Delta(t)^2} v \frac{d\Delta(t)}{dt} = i(t). \tag{36}$$

Now, if the voltage $v(t)$ is held at a constant value v_o, then the plate velocity is related to $i(t)$ by

$$\frac{d\Delta(t)}{dt} = -\frac{i(t)\Delta(t)^2}{\varepsilon_o A v_o}. \tag{37}$$

Thus, rate-feedback can be introduced by sensing the current $i(t)$ through a resistor in series with the capacitor as shown in Fig. 5. The current-sensing resistor can be attached directly to the bottom plate.

The proportional-plus-integral minor-loop controller can also be realized using operational amplifiers which can be integrated with the mirror assembly. Since the noninteracting controller requires algebraic manipulations, an external digital computer is needed for its implementation. However, it is possible to integrate this controller with the mirror assembly when single-chip specialized computers become available.

Finally, the wavefront estimator and the global mirror shape

controller require a digital computer with sufficiently high speed so that the processing time delay will not be detrimental to the performance of the overall system. Most likely, these components cannot be integrated with the mirror assembly.

To obtain some information on the orders of magnitude of various system parameters and variables, we consider a 1.7 mm square rectangular mirror with 15 × 15 actuator patches. Each patch is a 25 μm square pixel. The mirror membrane, leaf springs, and supporting posts are micromachined from single-crystal silicon sheets. Each leaf spring is a 45-μm long, 1-μm thick cantilever beam with rectangular cross-section (width = 4 μm). Using known data for single-crystal silicon [13] (Young's modulus E = 1.9 × 10^7 N/cm^2, and mass density ρ = 2.3 gm/cm^3), the electrostatic and spring forces associated with a single actuator can be computed from (6) and (7):

$$F_e \triangleq f_e A = 2.7669 \times 10^{-21}[V/(D - u)]^2 \text{ N} \tag{38}$$

$$F_s \triangleq f_s A = 8.340 \times 10^{-4} u \text{ N} \tag{39}$$

where V is the actuator voltage, D is in meters, and u is the tip displacement of the leaf spring in meters. For a square membrane with width L under uniform tension T, the upward restoring force on a square pixel with width ℓ located at the center of the membrane with a downward displacement u is given approximately by

$$F_T = 8T\ell u/L \text{ N}. \tag{40}$$

For T = 1 N/m, and the given dimensions for the membrane and pixels, (40) becomes

$$F_T = 0.11765u \text{ N}. \tag{40'}$$

For a typical membrane displacement u = 0.1 μm, and D = 0.5 μm, the required actuator voltage V can be computed by balancing the upward restoring forces F_s and F_T with the downward force F_e. The resulting V is equal to 0.8248 volt which is within the operating range of typical operational amplifiers.

Using the foregoing mirror parameters, the static actuator voltages V_{mn} for attaining a bi-parabolic mirror deformation are given by

$$u_d(x_1, x_2) = 1.9156 \times 10^{-13}(850^2 - x_1^2)(850^2 - x_2^2) \text{ μm}. \tag{41}$$

The results are shown in Fig. 6.

7. CONCLUDING REMARKS

In this paper, we have only considered the analytical design of a control system for a micromachined deformable mirror. The approach is to introduce first appropriate static feedback controls for noninteracting actuation. Both local rate-feedback and a minor-loop controller are introduced for modifying the dynamics of the actuators. Then a global controller is introduced for wavefront correction. Special consideration is taken to integrate the controllers with the mirror assembly. Other important factors such as thermal effects on the performance of the controlled deformable mirror are not studied here. The results pertaining to the fabrication of the proposed deformable mirror, and the actual

performance of the proposed control system are planned to be reported in the near future.

Acknowledgments

This work was performed at the Jet Propulsion Laboratory, California Institute of Technology, under contract with the National Aeronautics and Space Administration. The work of P.K.C. Wang was also supported in part by NSF Grant ECS 87-18473.

References

[1] J. Hecht, *Beam Weapons*, Plenum Press, New York, 1984.

[2] M.A. Ealey, "Active and Adaptive Optical Components: The Technology and Future Trends," *Adaptive Optics and Optical Structures*, R.K. Tyson and J. Schulte in den Bäumen, Editors, *Proc.SPIE*, Vol.1271, pp.2-34, 1990.

[3] R.K. Tyson, *Principles of Adaptive Optics*, Academic Press, 1991.

[4] R.P. Grosso and M. Yellin, "The Membrane Mirror as an Adaptive Optical Element," *J.Opt.Soc. Am.*, Vol.67, No.3, 1977, pp.399-406.

[5] J. Feinleib, S.G. Lipson, and P.F. Cone, "Monolithic Piezoelectric Mirror for Wavefront Correction," *Appl.Phys.Lett.*, Vol.25, pp.311-313, 1974.

[6] V.V. Apollonov *et al.*, "Magnetostrictive Actuators in Optical Design," *Active and Adaptive Optical Components*, M.A. Ealey, Editor, *Proc.SPIE*, Vol.1543, pp.313-324, 1991.

[7] W.G. Thorburn and L. Kaplan, "A Low Voltage Electrodistortive Mirror System for Wavefront Control," *Active and Adaptive Optical Components*, M.A. Ealey, Editor, *Proc.SPIE*, Vol.1543, pp.52-63, 1991.

[8] M.A. Ealey, "Precision Electrodisplacive Microactuators," *Precision Engineering and Optomechanics*, D. Vukobratovich, Editor, *Proc.SPIE*, Vol.1167, pp.85-102, 1989.

[9] M.A. Ealey and J.F. Washeba, "Continuous Facesheet Low Voltage Deformable Mirrors," *Opt.Engr.*, Vol.29, No.10, 1990, pp.1191-1198.

[10] L.J. Hornbeck, "128 × 128 Deformable Mirror Device," *IEEE Trans. Electron Devices*, Vol.ED-30, No.5, pp.539-545, 1983.

[11] M.A. Ealey and C.E. Wheeler, "Integrated Wavefront Corrector," *Adaptive Optics and Optical Structures*, R.K. Tyson and J. Schulte in den Bäumen, Editors, *Proc.SPIE*, Vol.1271, pp.254-264, 1990.

[12] D.L. Fried, "Least Square Fitting a Wavefront Distortion Estimate to an Array of Phase Difference Measurements," *J.Opt.Soc.Am.*, Vol.67, pp.370-375, 1977.

[13] K.E. Petersen, "Silicon as a Mechanical Material," *Proc.IEEE*, Vol.70, No.5, pp.420-457, 1982.

APPENDIX

Explicit expressions for K_s and p_{mn}^{ij} corresponding to rectangular and circular mirrors are given below.

For a rectangular mirror with spatial domain $\Omega = \Omega_R \triangleq \{(x_1,x_2) \in R^2: |x_i| < \ell_i,\ i = 1,2\}$ and uniform tension T, the Green's function K_s is given by

$$K_s(x_1,x_2,x_1',x_2') = \sum_{k=1}^{\infty}\sum_{k'=1}^{\infty} \frac{4\ell_1\ell_2}{\pi T(k^2\ell_1^2 + k'^2\ell_2^2)} \sin\left(\frac{k\pi(x_1+\ell_1)}{2\ell_1}\right)\sin\left(\frac{k\pi(x_2+\ell_2)}{2\ell_2}\right)$$
$$\times \sin\left(\frac{k'\pi(x_1'+\ell_1)}{2\ell_1}\right)\sin\left(\frac{k'\pi(x_2'+\ell_2)}{2\ell_2}\right). \tag{A1}$$

Let the actuator patches Ω_{mn} be square pixels with width Δ. Thus $\Omega_{mn} = \{(x_1,x_2) \in R^2: |x_1 - x_{1m}| < \Delta/2,\ |x_2 - x_{2n}| < \Delta/2\}$. Assuming that the actuator weighting function ϕ_{mn} corresponds to the characteristic function of Ω_{mn} (i.e. $\phi_{mn}(\mathbf{x}) = 1$ if $\mathbf{x} \in \Omega_{mn}$, and $\phi_{mn}(\mathbf{x}) = 0$ otherwise), the coefficients p_{mn}^{ij} defined by (17) are given by

$$p_{mn}^{ij} = \frac{\varepsilon_o}{2(D - u_d(\mathbf{x}_{mn}))^2} \sum_{k=1}^{\infty}\sum_{k'=1}^{\infty} \frac{4\ell_1\ell_2\alpha_{mk'}\beta_{nk'}}{\pi T(k^2\ell_1^2 + k'^2\ell_2^2)}$$
$$\times \sin\left(\frac{k\pi(x_{1i}+\ell_1)}{2\ell_1}\right)\ \sin\left(\frac{k\pi(x_{2j}+\ell_2)}{2\ell_2}\right), \tag{A2}$$

where $\mathbf{x}_{ij} = (x_{1i},x_{2j})$, and

$$\alpha_{mk'} = \int_{x_{1m}-\Delta/2}^{x_{1m}+\Delta/2} \sin\left(\frac{k'\pi(x_1'+\ell_1)}{2\ell_1}\right) dx_1' = \frac{2\ell_1}{k'\pi}\left\{\cos(k'\pi(x_{1m} - \frac{\Delta}{2} + \ell_1))\right.$$
$$\left. - \cos(k'\pi(x_{1m} + \frac{\Delta}{2} + \ell_1))\right\}, \tag{A3}$$

$$\beta_{nk'} = \int_{x_{2n}-\Delta/2}^{x_{2n}+\Delta/2} \sin\left(\frac{k'\pi(x_2'+\ell_2)}{2\ell_2}\right) dx_2' = \frac{2\ell_2}{k'\pi}\left\{\cos(k'\pi(x_{2n} - \frac{\Delta}{2} + \ell_2))\right.$$
$$\left. - \cos(k'\pi(x_{2n} + \frac{\Delta}{2} + \ell_2))\right\}. \tag{A4}$$

The Green's function K_s for a circular mirror with spatial domain $\Omega_c = \{(r,\theta),\ 0 \le r \le r_o,\ 0 \le \theta \le 2\pi\}$ and uniform tension T is given by

$$K_s(\theta,r,\theta',r') = \sum_{k=1}^{\infty}\sum_{k'=1}^{\infty} \frac{2}{\pi T r_o^2 [J_{k+1}(\lambda_{kk'}r_o)]^2} J_k(\lambda_{kk'}r)[J_{kk'}(\lambda_{kk'}r')\cos(k\theta)$$

$$\times \cos(k\theta') + J_{kk'}(\lambda_{kk'}r')\sin(k\theta)\sin(k\theta')], \tag{A5}$$

where J_k denotes the Bessel function of the first kind of order k, and $(\lambda_{kk'}r_o)$ is k'-th zero of J_k.

Let the actuator patches Ω_{mn} be fan-shaped pixels with radial length Δ and aperture angle θ_p as shown in Fig. 3. Thus $\Omega_{mn} = \{(\theta,r): |\theta - \theta_m| < \theta_p/2, |r - r_n| < \Delta/2\}$. In this case, the coefficients p_{mn}^{ij} defined by (17) with ϕ_{mn} being the characteristic function of Ω_{mn} are given by

$$p_{mn}^{ij} = \frac{\varepsilon_o}{2(D - u_d(\mathbf{x}_{mn}))^2} \sum_{k=1}^{\infty}\sum_{k'=1}^{\infty} \frac{2}{\pi T r_o^2 [J_{k+1}(\lambda_{kk'}r_o)]^2} J_k(\lambda_{kk'}r_j)$$

$$\times [\hat{\alpha}_{mk'}\cos(k\theta_i) + \hat{\beta}_{nk'}\sin(k\theta_i)], \tag{A6}$$

where

$$\hat{\alpha}_{mk'} = \left\{\int_{\theta_{mk'}-\theta_p/2}^{\theta_{mk'}+\theta_p/2} \cos(k'\theta')\, d\theta'\right\} \left\{\int_{r_m-\Delta/2}^{r_m+\Delta/2} J_{kk'}(\lambda_{kk'}r')\, r'dr'\right\}, \tag{A7}$$

$$\hat{\beta}_{nk'} = \left\{\int_{\theta_{nk'}-\theta_p/2}^{\theta_{nk'}+\theta_p/2} \sin(k'\theta')\, d\theta'\right\} \left\{\int_{r_n-\Delta/2}^{r_n+\Delta/2} J_{kk'}(\lambda_{kk'}r')\, r'dr'\right\}. \tag{A8}$$

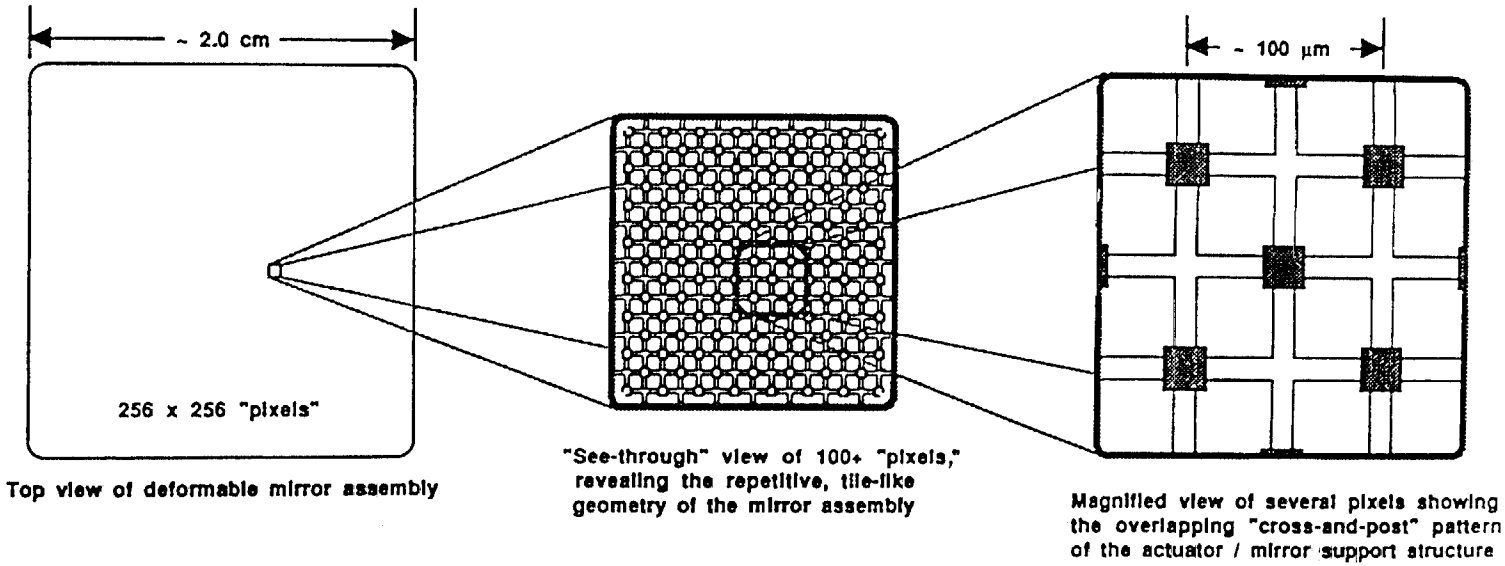

Fig. 1 Top view of the deformable mirror.

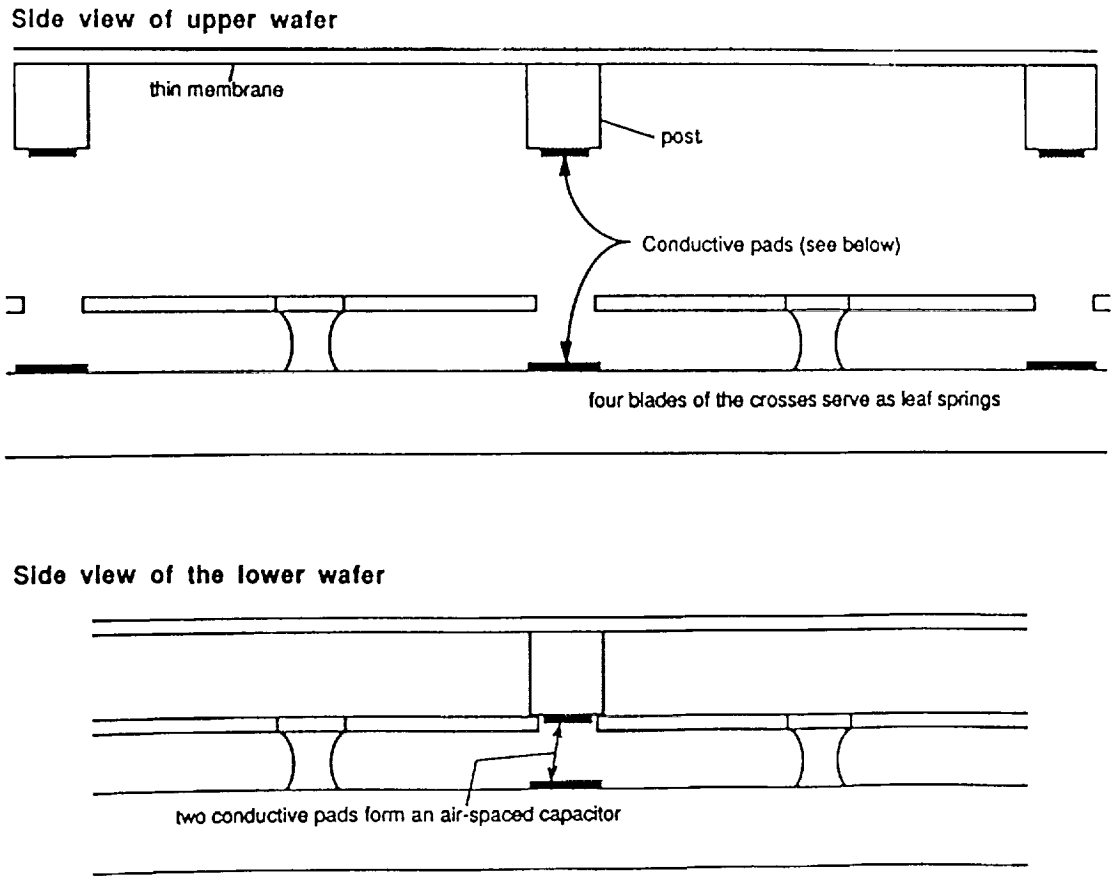

Fig.2 Side view of the deformable mirror.

RECTANGULAR MIRROR: $\Omega_R \triangleq \{(x_1, x_2) \in R^2: |x_1| \leq \ell_1, |x_2| \leq \ell_2\}$,

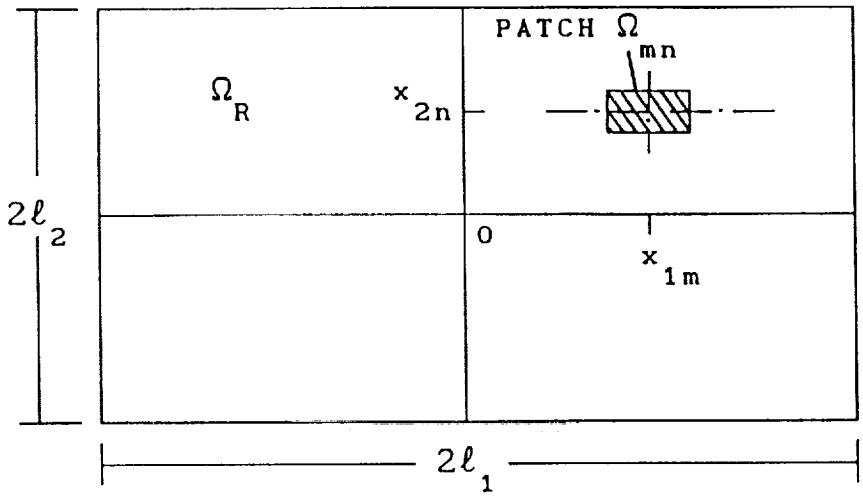

CIRCULAR MIRROR: $\Omega_c \triangleq \{(r, \theta),\ 0 \leq r \leq r_o,\ 0 \leq \theta \leq 2\pi\}$.

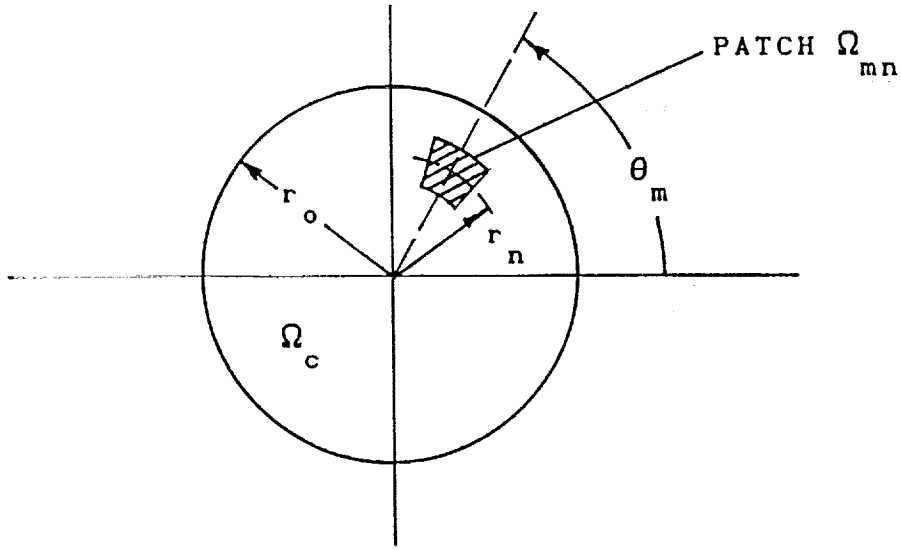

Fig. 3 Typical meshes and patches for rectangular and circular Mirrors.

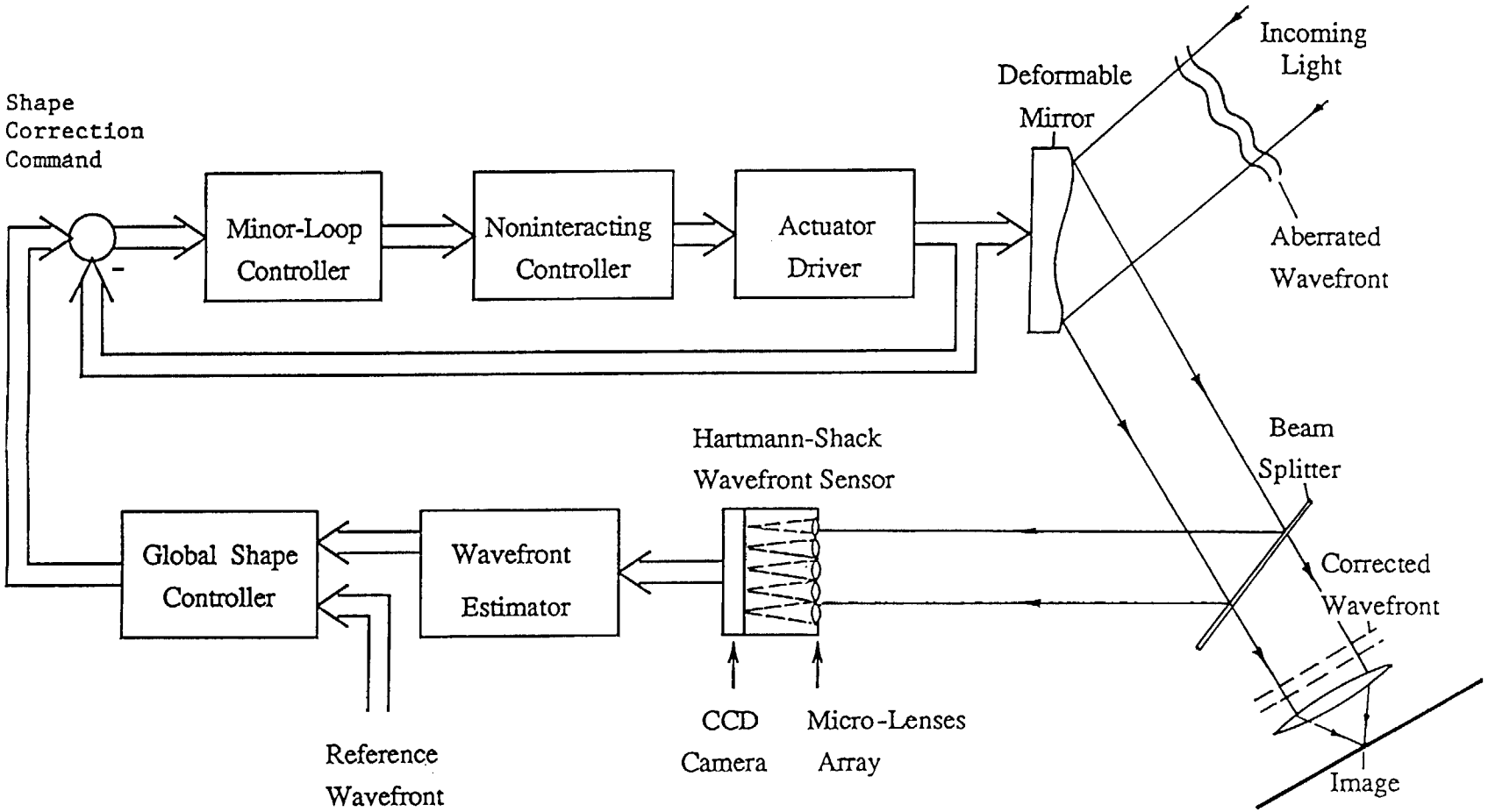

Fig. 4 Structure of the overall control system for wavefront correction.

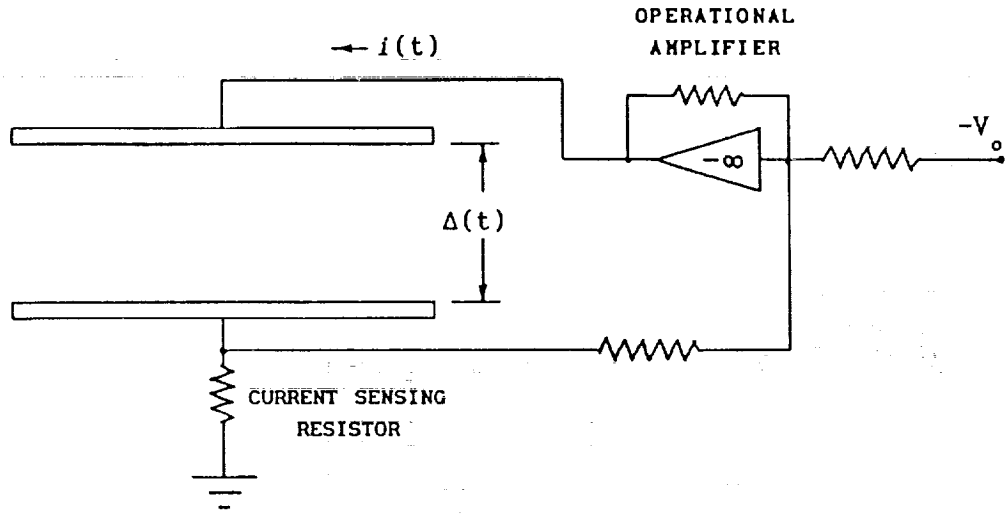

Fig.5 Implementation of local rate-feedback control.

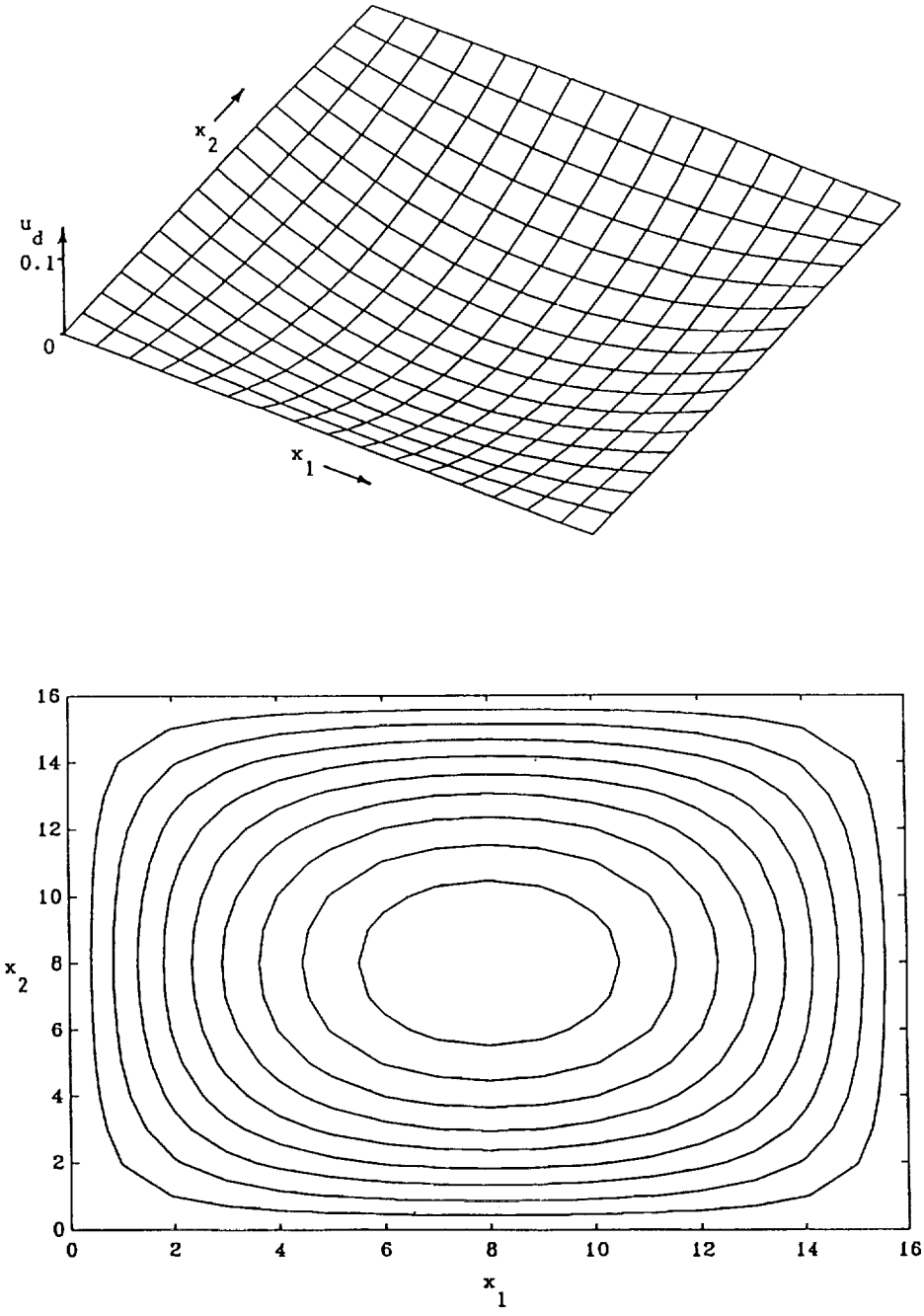

Fig. 6a Desired bi-parabolic deformation u_d for a 1.7 mm square mirror with 15 × 15 actuators. (Minimum deformation at mirror center = 0.1 μm.)

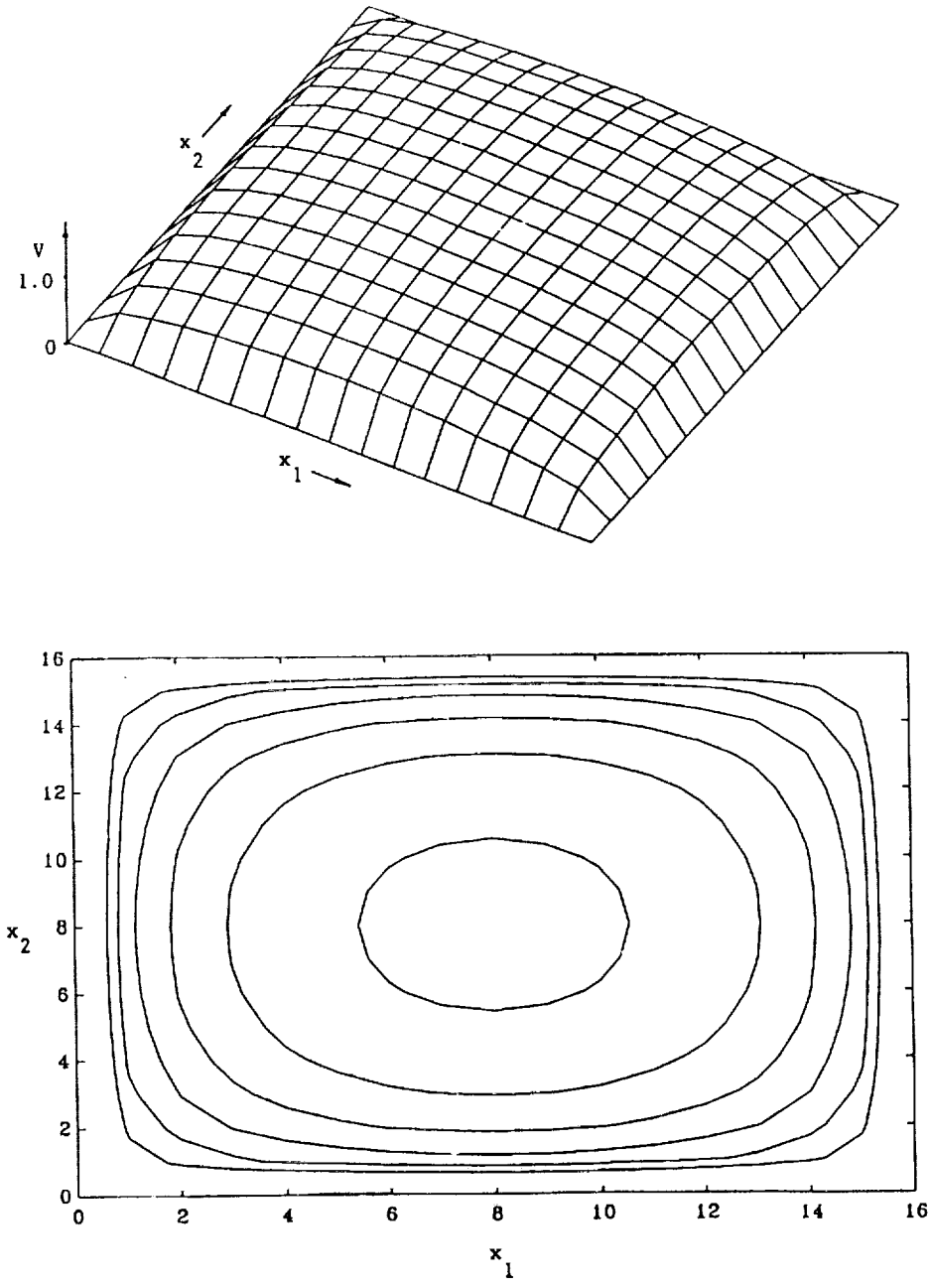

Fig. 6b Required static actuator voltages V_{mn} for bi-parabolic mirror deformation given in Fig. 6a. (Maximum voltage at mirror center = 0.8248 volt.)